Age-related phenological and anatomical response of European beech (*Fagus sylvatica* L.) under severe summer drought conditions

Dimitrios Tsalagkas*, Hanuš Vavrčík, Vladimír Gryc, Kyriaki Giagli

Department of Wood Science, Faculty of Forestry and Wood Technology, Mendel University in Brno, Brno, Czech Republic

*Corresponding author: dimitrios.tsalagkas@mendelu.cz

Citation: Tsalagkas D., Vavrčík H., Gryc V., Giagli K. (2024): Age-related phenological and anatomical response of European beech (*Fagus sylvatica* L.) under severe summer drought conditions. J. For. Sci., 70: 458–475.

Abstract: The year 2018 was distinguished by a warm summer with extended periods of low or no precipitation. In this context, we investigated the intra-annual dynamics of xylem differentiation phases and quantitative vessel anatomy to analyse the age effect on the xylem formation response of younger (50 years) and older (135 years) mature European beech trees under summer drought conditions. The xylem formation dynamics of young and old trees were performed on microcores collected at weekly intervals in the Rájec-Němčice ecological station in the South Moravia region (Czech Republic). The onset of xylem formation was found identical in both age trees, and most of the trees ceased their enlargement by the end of July, which is attributed to the harsh environmental conditions of this month. Young trees were characterised by a 10-day extended enlargement period and a higher growth rate, resulting in more vessels and a wider tree-ring width. No significant linkage was found between intra-annual environmental conditions of the 2018 year or age effect and the vessel anatomy traits.

Keywords: climate change; vessel morphology; wood formation; xylem phenology; xylogenesis

As trees grow seasonally in temperate regions, xylem formation (or xylogenesis) occurs periodically as an annual, highly dynamic process regulated by several intrinsic and environmental factors (Battipaglia et al. 2014). Tree species adjust their xylem phenology response to climate according to specific regional environmental drivers, local adaptations, and individual plasticity by shifting their cambial activity, tree-ring growth and cell anatomy (Vieira et al. 2020). Therefore, the phenotypical plasticity of tree populations indicates their adaptive capacity under a changing environment, and it is ex-

pected to influence xylem formation and tree-ring growth (Matisons et al. 2019). Variability in xylem anatomy through quantitative analysis, in combination with valuable information on the xylem formation and factors affecting it, offers a more holistic approach to trees' ecophysiological response to extreme weather events or contrasting environments (Diaconu et al. 2017; Deslauriers et al. 2018) and predicting questions relevant to other disciplines such as forest ecology and forest management (Beeckman 2016) or even the probability of tree mortality (Cailleret et al. 2017).

Supported by funding from the Internal Grant Agency (IGA) of the Faculty of Forestry and Wood Technology at Mendel University in Brno under Grant Agreement No. IGA-LDF-22-IP-034.

[©] The authors. This work is licensed under a Creative Commons Attribution-NonCommercial 4.0 International (CC BY-NC 4.0).

Fagus sylvatica trees present an intensive, shallow fine root system that hampers water uptake during drought, making them sensitive to drought episodes (Charru et al. 2010; Eilmann et al. 2014). A warmer climate, with frequent heat waves and summer droughts, might substantially impact F. sylvatica vessel anatomy since in broadleaves, the water-conducting system is principally determined by the size, the number and the spatial arrangement of the vessels (Diaconu et al. 2016). Internal factors in Fagus species are effective mainly during the initial phase of wood formation, by producing wider vessels at the beginning because of the vital necessity for water supply in the xylem growth. Later in the growing season, more and narrower vessels occur, where external factors such as environmental conditions probably become more influential (Sass, Eckstein 1995; Pourtahmasi et al. 2011).

Hence, as a tree matures in age, it presents an evident growth decline accompanied by physiological changes leading to carbon assimilation and resource economy reduction (Genet et al. 2010). Post-juvenile changes, after the first 50–100 years of a tree's life during the ageing process in trees, imply a shortening of the growing period and a progressive reduction in the growth rates with narrower tree rings, thus a reduced amount of produced wood (Dorado-Liñán et al. 2012). Diaconu et al. (2016) indicated that tree-ring width (*TRW*) is the driving force that controls xylem plasticity in *F. sylvatica* trees since the *TRW* mainly controls variations in different vessel traits.

According to other studies in conifer trees, the timing and duration of xylem development vary as the tree matures. Older trees require fewer days for xylem differentiation and produce fewer cells, indicating that tree age influences the timing and duration of growth (Rossi et al. 2008; Li et al. 2013; Zeng et al. 2018). Furthermore, ageing issues arise if the kinetics of the vascular cambium, xylem formation, and cell anatomy of the young mature trees respond differently from that of the old mature trees under the impact of regional and local climatic and environmental stresses (Čermák et al. 2019; Rodriguez-Zaccaro et al. 2019). Current knowledge on xylem formation monitoring has been concentrated on conifer species, yet broadleaved species with varying anatomical cells exhibit different physiological and adaptation needs to the environmental conditions (Chen et al. 2022).

F. sylvatica trees have been recorded to face increased mortality rates or dieback episodes on some shallow soils during exceptional heatwaves and drought episodes, such as the 2018/2019 drought (Leuschner 2020). In 2018, temperate forests of central European countries experienced one of the most intense and long-lasting summer droughts and heat waves, with parts of this region receiving less than 50% of the long-term mean precipitation, leading to severe water deficits with grave consequences (Boergens et al. 2020). Notably, in 2018, the Czech Republic recorded (i) a rapid onset of the spring season with monthly mean temperatures above the long-term mean, (ii) a warm and dry summer with extended periods of little or no precipitation, and (iii) a total annual precipitation deficit of over 30% (Skalák et al. 2019).

Although the xylem growth formation and anatomy of F. sylvatica trees have been studied on different sites in Europe (del Castillo et al. 2016), studies along the age effect on vessel anatomy are still missing. We investigated the xylem phenology and vessels' anatomical traits formed in 2018 on two age-class mature F. sylvatica forest stands to address this knowledge gap. As for the effect of age on radial growth, we expect that the younger age F. sylvatica trees (i) will display higher growth rates, wider xylem (TRW) increments and a longer growing period (H₁) (Ryan et al. 1997; Dorado-Liñán et al. 2012), and (ii) different timing and duration of xylem formation phenological phases as has been observed in conifer species (H_2) . The main aim of this study was to examine the intra-annual differences in the xylem phenology and vessels' anatomical traits in mature F. sylvatica trees due to the effect of age during a severe climatic event, such as that of 2018 year.

MATERIAL AND METHODS

Site characteristics. The measurements were carried out in 2018 in two mature *F. sylvatica* stands of different ages (50 and 135 years old) in the South Moravian region, in the hills of Drahanská highlands. *F. sylvatica* trees were growing at the Rájec-Němčice (RAJ) ecological station (49°26'N, 16°41'E) in a low-elevation (~ 625 m a.s.l.) forest area, classified as 5S1 – *Abieto-Fagetum mesotrophicum* forest type (Urban et al. 2014). The geological bedrock consists of acidic granodiorite, while the main soil type is loam-clay cambisols, with a shal-

low soil depth ranging around 40–70 cm (McGloin et al. 2019). The RAJ is part of the Czech long-term ecosystem research network (https://lter.cz/en/homepage), the Czech Carbon Observation System (CzeCOS) network (http://www.czecos.cz/en.html) and the Integrated Carbon Observation System (http://www.icos-cp.eu) international network (Chawla et al. 2018). From a climatic point of view, according to the Köppen classification, the largest part of the Czech territory falls into the category of temperate broadleaf deciduous forests, generally influenced by the effects of the Atlantic Ocean, the Mediterranean and Eurasia (Brázdil et al. 2021).

Weather data. The region of RAJ, located in the Brno region, experiences a moderately warm and humid climate with low annual precipitation (Kolář et al. 2016). The EURO-CORDEX database results further show that the values of summer climate indices in all the Brno regional climate zones will significantly increase towards the twenty-first century's first decade (Geletič et al. 2019).

To characterise the weather conditions of the year 2018 thoroughly, we used both environmental variables and a broadly used bioclimatic index as a meteorological drought indicator. Continuous measurements of the relative humidity (RH; Minikin TRH; EMS Brno, Czech Republic), air temperature ($T_{\rm air}$; Minikin TRH; EMS Brno, Czech Republic), precipitation sum (PRCP; 360 Precipitation Gauge; MetOne Instruments, USA) and soil water content (SWC; GB-2; Delmhorst Towaco, USA, attached to an SP3 data logger; EMS Brno, Czech Republic) were performed directly on the study site.

The vapour-pressure deficit (VPD) reflects the effect of $T_{\rm air}$ and PRCP on RH and transpiration demand. It is often monitored as a proxy for plant water stress, stimulating stomatal closure and photosynthetic carbon fixation (Broz et al. 2021). Above-ground atmospheric demand for moisture was represented by the VPD (kPa), according to Equation (1):

$$VPD = \left(1 - \frac{RH}{100}\right) \times SVP \tag{1}$$

where:

VPD – vapour-pressure deficit;

RH – relative humidity;

SVP – saturated vapour pressure for a given temperature (kPa).

SVP was estimated according to Teten's equation – see Equation (2) below (Hoylman et al. 2019):

$$SVP = 0.61078 \times exp \left(\frac{17.27 \times T_{air}}{T_{air} + 237.3} \right)$$
 (2)

where:

 $T_{\rm air}$ – temperature (°C).

The year 2018 was distinguished by a warm but not exceptionally dry spring (April–June) followed by an arid period during the summer months (July–August), see Figure 1. In addition, extremely low RH values and increased $T_{\rm air}$ and VPD values characterised the June–August months of 2018.

The acquired meteorological data was subsequently compared with the long-term monthly archive data for the period 1961-2022 obtained from the nearest Czech hydrometeorological station (Protivanov, ID: B1PROT01; ~ 675 m a.s.l.; 49°29'N, 16°50'E), as provided by the Czech Hydrometeorological Institute (www.chmi.cz). The annual PRCP for the year 2018 was 474.6 mm, 26% less relevant to the 1961-2022 long-term period (643.4 mm), while July-August PRCP was only 42.6 mm (minus 73%) compared to the 158.7 mm in the same period (1961-2022). The mean annual $T_{\rm air}$ was 8.8 °C and 6.8 °C for 2018 and 1961–2022, respectively. Similarly, the $T_{\rm air}$ during the growing season (April to August) was 16.8 °C and 13.2 °C for the 2018 and the long-term period, i.e. in 2018, it was 3.6 °C higher (Table 1).

Even more, based on the monthly temperature and precipitation data, we quantified the meteorological drought according to the Standardised Precipitation-Evapotranspiration Index (SPEI), according to Vicente-Serrano et al. (2010). This index counted and computed the difference between precipitation and potential evapotranspiration using the Thornthwaite equation (R package SPEI, Version 4.2.3) for the 2010–2020 period. A resolution of only one month was chosen to cover short drought episodes since short-time drought events might affect drought-sensitive tree species such as F. sylvatica (Leuschner 2020), as Fonti and Babushkina (2016) proposed. We adopted the drought intensity assessment that Parente et al. (2019) employed to characterise the drought events based on the SPEI drought index (DI). The drought intensity conditions were classified into four classes as follows: (i) mild $(-1.0 < DI \le 0)$, (ii) moderate

Apr

May

- PRCP

https://doi.org/10.17221/16/2024-JFS

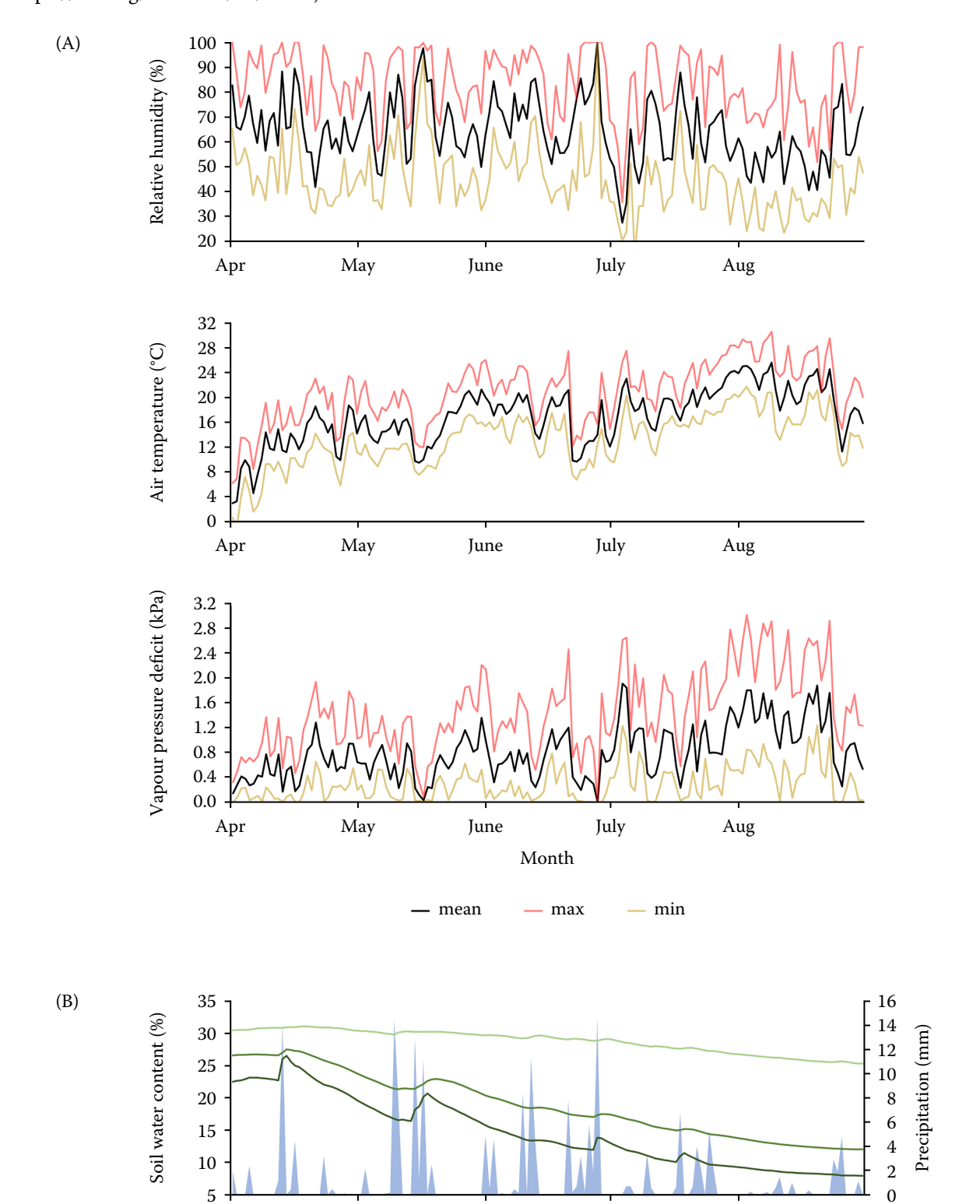


Figure 1. (A) Daily mean, maximum (max), and minimum (min) air temperature ($T_{\rm air}$, °C), relative humidity (RH, %), and vapour-pressure deficit (VPD, kPa) for the Rájec-Němčice ecological station; and (B) daily mean soil water content (SWC, %) at 0.05, 0.2, and 0.8 m depths and precipitation sum (PRCP, mm) during the growing season (April–August 2018)

June

— SWC 0.05 m

Month

July

— SWC 0.2 m

Aug

— SWC 0.8 m

Table 1. Differences in the mean monthly air temperature (T_{air}) and precipitation sum (PRCP) between the year 2018 (Rájec-Němčice ecological station) and the long-term weather data (1961–2022) in the Protivanov station

Meteorological parameters		Jan	Feb	Mar	Apr	May	June	July	Aug	Sept	Oct	Nov	Dec
	1961-2022	-3.5	-2.1	1.5	6.6	11.5	14.8	16.6	16.4	12.2	7.3	1.9	-2.2
$T_{\rm air}$ (°C)	2018	-0.1	-4.8	-0.5	12.2	15.4	16.7	19.1	20.8	14.8	10.0	3.7	-1.2
	difference	+3.4	-2.7	-2.0	+6.1	+3.9	+1.9	+2.5	+4.4	+2.6	+2.7	+1.8	+1.0
DD GD	1961-2022	33.7	31.7	39.1	43.1	74.3	82.8	81.0	77.7	56.1	44.2	42.8	36.9
PRCP (mm)	2018	62.3	21.5	25.6	28.3	52.8	69.6	27.8	14.8	72.2	25.4	23.5	50.8
	difference	+28.6	-10.2	-13.5	-14.8	-21.5	-13.2	-53.2	-62.9	+16.1	-18.8	-19.3	+13.9

 $(-1.5 < DI \le -1.0)$, (*iii*) severe $(-2.0 < DI \le -1.5)$, and (*iv*) extreme ($DI \le -2.0$).

According to *SPEI*, a drought event is distinguished as a period in which the *SPEI* value is below the negative threshold level of -1.0 and is described by its severity, duration, and frequency (Mesbahzadeh et al. 2020). In this study, we used 2015–2020 as a reference period to quantify the drought conditions that occurred during 2018. As illustrated in Figure 2, the second half of the year 2018 displayed the most severe and intense dry conditions compared to the reference period (2015–2020).

Tree sampling and preparation. We randomly selected 12 dominant and co-dominant vital *F. sylvati*-

ca trees without any visible marks of stem and crown damage. Two age classes of F sylvatica stands were defined, and six trees per stand (i.e. age class) were chosen on the RAJ, resulting in young and old trees with an average cambial age of ca. 50 and 135 years, respectively. The mean diameter at breast height was 23.8 cm \pm 2.0 cm and 38.8 cm \pm 3.4 cm for the young and old trees, respectively.

Sampling for xylem formation (i.e. xylogenesis) monitoring was performed from April to November 2018, collecting microcores on the stem weekly with a Trephor tool (patent No. PD2004A000324, Italy; Rossi et al. 2006). Two microcores were collected from 30 cm below and above breast height

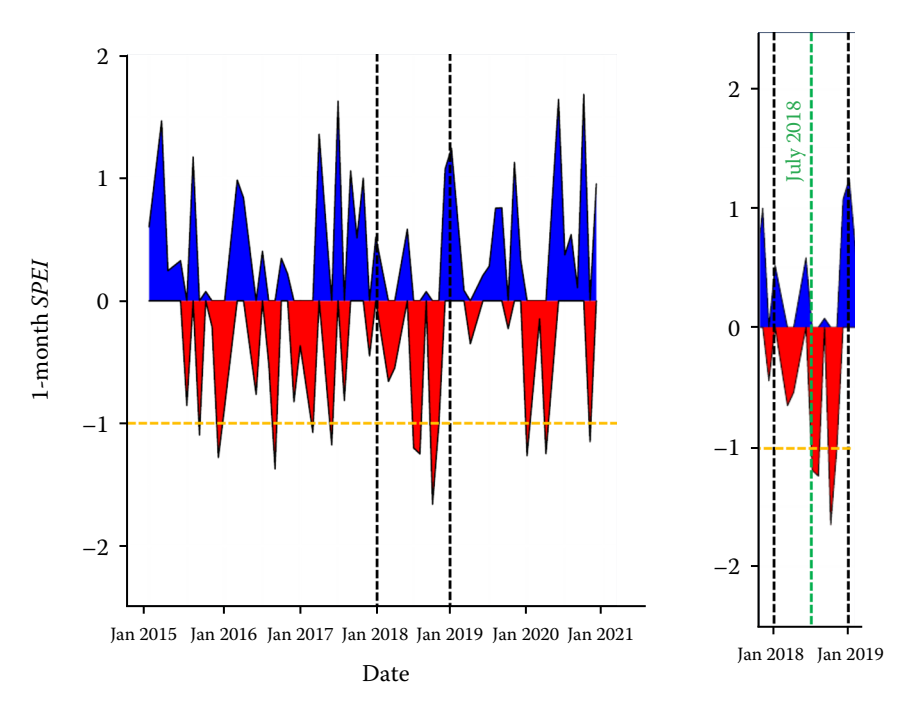


Figure 2. One-month Standardised Precipitation-Evapotranspiration Index (1-month *SPEI*) at the Rájec-Němčice experimental ecological station for 2015–2020

Black dashed lines – boundaries of 2018; yellow dashed line – negative threshold value of -1.0; green dashed line – start of the second half-period of 2018, i.e. July–December

in a spiral pattern, at least 5 cm apart, to prevent wood defects from adjacent sampling points. Each microcore contained phloem, vascular cambium, and at least two of the last formed xylem growth rings (Prislan et al. 2013). Microcoring has been adopted as the main technique for sampling and monitoring intra-annual wood formation dynamics (De Micco et al. 2019).

Immediately after removal from the standing trees, the microcores were placed in histosettes and stored in ethanol-formalin acetic acid solution for a week (Prislan et al. 2013; Prislan et al. 2022). The microcores were dehydrated in the laboratory through successive immersions in ethanol solutions and Bio-Clear (Bio-Optica, Italy) and embedded in paraffin blocks. Transverse sections of 12 µm thickness were cut from the embedded microcores with a rotary microtome RM2235 (Leica Microsystems, Germany), using Feather N35H (Feather Razor Safety Co., Japan) microtome blades. The microsections were then transferred to microscope slides and, after a paraffin washing procedure, were stained with a safranin (Merck S.A., Germany), astra blue (Sigma-Aldrich Chemie GmbH, Germany) water solution and finally were permanently mounted in Euparal (Waldeck GmbH & Co, Germany). Histometrical analyses were performed on images taken with a Leica DM 2000 microscope equipped with polarised light and connected to a Leica DFC 295 digital camera (Leica Microsystems, Germany).

Xylem formation monitoring. Current research on seasonal intra-annual dynamics of a xylem formation process can be divided into the following five separated but also overlapping major phases during a tree-ring growth: (i) the periclinal division of a cambial mother cell into daughter cells, (ii) the increase in size and enlargement of the daughter cells, (iii) the deposition of different layers of secondary cell wall, (iv) secondary cell wall lignification, and (v) programmed cell death (Plomion et al. 2001; Cartenì et al. 2018). This sequence is common to both angiosperms and gymnosperms (Rathgeber et al. 2016). Xylem formation depicts the production of new cell derivatives in a radial file along with temporal succession differentiation phases, undergoing a spatial pattern of differentiation strips (Rathgeber et al. 2018). Thus, xylem formation is a complex spatial-temporal developmental process involving cambium activity, cell division and differentiation of secondary xylem (Hartmann et al. 2017).

Xylem formation monitoring studies are generally established on a broadly used conceptual model developed by Wilson et al. (1966) describing xylem cell formation as the succession of four differentiation phases (Rathgeber et al. 2018; De Micco et al. 2019): (i) cell division (division of cambial mother cells), (ii) cell enlargement (newly formed cells expanding in the radial direction), (iii) cell wall thickening (secondary walls are built and cell walls are lignified), and (iv) mature cells (programmed cell death, i.e. autolysis of the cytoplasm marks the end of cell differentiation and the advent of an empty, fully functional tracheary element). Briefly, the phenology of xylem growth is defined as the timing of the physiological phases that occur during the seasonal formation of wood, starting with cambial reactivation and ending with the lignification completion (Dox et al. 2022).

Anatomical observation of xylem formation monitoring. Experimentally, the developmental zone phases are defined based on similar visual criteria, attributing 'apparent status' to virtual cells (Hartmann et al. 2017). We associated the four conceptual phases of xylem cell differentiation (cambial dividing zone, cell enlarging zone, wall thickening zone and mature zone) according to criteria reviewed by Rossi et al. (2006), Oladi et al. (2011), Prislan et al. (2013), del Castillo et al. (2016), and Dox et al. (2021). For angiosperms, the widths of the four differentiation zones are measured (De Micco et al. 2019). Likewise, this study measured the tree-ring widths of the developing xylem increments for three radial files in each histological section per tree to evaluate the dynamics of xylem growth ring formation.

In cross-sections, cambial cells in the cambial zone are distinguished as radially small diameter flattened cells, presenting thin, primary cell walls that are not birefringent under polarised light (Čufar et al. 2008; Rathgeber et al. 2011). During winter, the dormant cambium (Figure 3A) is characterised by a few layers of cells, while the active cambium comprises numerous dividing cells (Figure 3B). A couple of days or weeks later after the start of cambial activity (Figure 3B), the appearance of the first post-cambial cells (enlarging phase) is visible, still consisting only of primary thin cell walls, not birefringent under polarised light, but larger in radial diameter (Prislan et al. 2013; Rathgeber et al. 2016).

After cambial cell division, cells enter the differentiation zone, turning into either xylem or phloem

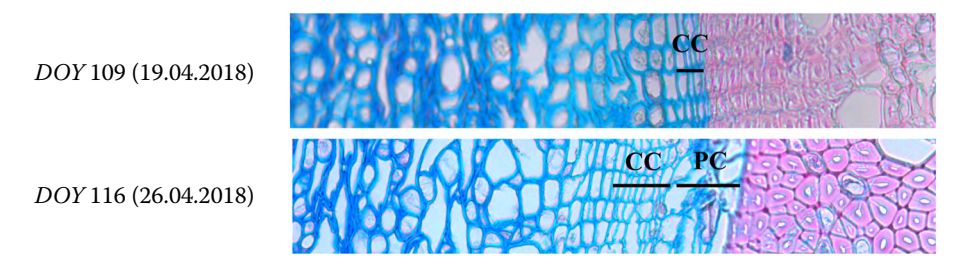


Figure 3. Beginning of xylem ring formation in European beech (*Fagus sylvatica*): Cambial cells (CC) and post-cambial cells (PC) growth on April 19 (phase of dormancy) and April 26 (activated cambial zone and enlarging phase), 2018 *DOY* – day of the year

cells. The formed cells follow the abovementioned successive developmental differentiation phases till they become fully mature and conductive cells. The presence of the first enlarging cells indicates the beginning of xylem growth and cambial cell production. A couple of days or weeks later, the cells become thicker and start forming their secondary walls. A couple of weeks or months later, the cells reach their mature phase (thickened, lignified secondary cell walls with an empty lumen), reaching their functional purpose as conducting xylem tracheary elements (Rathgeber et al. 2016) in the case of the vessels. This is a dynamic continuous process through the whole growing season, since cells in the same radial file can be at separated phases of differentiation (Rathgeber et al. 2011; Rossi et al. 2006).

The polarised light enabled the distinction between enlarging cells, secondary wall thickening cells and mature cells as described in Oladi et al. (2011), Gričar et al. (2014), del Castillo et al. (2016), and Dox et al. (2021). Under polarised light, the deposition of secondary walls appears bright (birefringent), recognisable by a blue cell wall, whereas cambial and post-cambial growth cells remain dark. Secondary wall thickening starts at the cessation of cell enlargement. Observing the first woody cells with partly red-coloured walls was considered the start of lignification. Cessation of xylem differentiation was distinguished by the complete lignification of a cell, when a cell wall became entirely red through the safranin-Astra blue staining, and the cell was considered mature, having a homogeneous dark-red-coloured wall and an empty lumen.

Even though the beginning, duration and cessation of cambial activity are weighty information, they cannot be accurately defined (Rathgeber et al. 2018). However, at the end of the growing

season, cell division cessation is shortly followed by cell enlargement cessation, indicating the end of radial xylem growth and, accordingly, the cessation of cambial activity (Rathgeber et al. 2016). Thus, the cessation and duration of cambial cell enlargement are considered the cessation of cambial activity and cambial cell production period (Dox et al. 2021). Cessation of cambial cell production is identified as the time at which no new thin-walled cells were observed adjacent to the cambium, and the number of cambial cells was similar to the number of cambial cells in the dormancy (Gričar et al. 2014).

Definition of xylem formation critical dates. Typical elaborated analysis of the raw anatomical data in the field of xylem monitoring is performed on critical dates and durations of xylem formation extracted from the four conceptual phases of xylem differentiation (Rathgeber et al. 2018). Critical dates, i.e. days of the years (DOY) of each phenological phase of xylem formation (Rathgeber et al. 2011; Prislan et al. 2019) were recorded as (i) the beginning of cell enlargement (bE), (ii) the beginning of secondary wall thickening, which corresponds to the first appearance of secondary wall thickening in the formed vessels (bW), (iii) the beginning of mature vessels, which corresponds to the appearance of the first mature vessels (bM), (iv) the cessation of cambial cell production, which corresponds to the cessation of cell enlargement (cE), and (ν) the cessation of xylem cell differentiation which corresponds to the end of secondary wall thickening and lignification (cW). Subsequently, based on the DOY, the following critical durations of the xylem formation process were further estimated: (i) the overall duration of the enlargement period (dE = cE - bE), i.e. the duration of cambial cell production, (ii) the duration of the secondary wall thickening period (dW = cW - bW), and (iii) the

total duration of xylem formation (dX = cW - bE) (D'Andrea et al. 2020; Larysch et al. 2021).

Xylem formation modelling. For temperate forest trees, the accumulation along the growing season of xylem cells in the forming ring is described using a Gompertz function (Rathgeber et al. 2018). The Gompertz function has been used intensively to model tree-ring growth (Deslauriers et al. 2003) since temporal xylem cells series measurements follow a sigmoidal shape and a final asymptote maximal plateau at the end of the growing period (Kraus et al. 2016). To assess daily and weekly relationships between xylem growth and the environment, intraannual dynamics of cell differentiation phase timings were fitted to the Gompertz function of the xylem width increments (Rossi et al. 2003), using the curve Fityk software (GNU General Public License, Version 2.0, 2016), according to Equation (3):

$$y = A \times e^{-e^{(\beta - k \times t)}} \tag{3}$$

where:

y — the total xylem ring width (μ m) at time t, in this study representing the weekly cumulative width;

A – the final upper asymptotic size representing the annual potential growth;

he x-axis placement parameter, representing the onset of cambial activity;

k – the parameter of growth rate change;

t – time expressed in *DOY*.

The maximum growth rate of xylem cell production was calculated using the Gompertz function equation, marked at the inflection point of the sig-

moidal point curve (Prislan et al. 2013). The first derivatives of Gompertz functions were used for comparing the daily xylem increment values with the theoretical incremental xylem formation during the growing season (Ježík et al. 2016) and detect the differences in the rate of xylem cell production in each stand (Gričar et al. 2014).

Quantitative wood anatomy. The TRWs of the fully formed xylem increments were measured and then divided into four equal domains (Q1, Q2, Q3, and Q4) to compare vessel variability between the vessels formed during the growing season of the year 2018. The vessel anatomical traits were counted on each microsection domain using the ImageJ's image processing software (Version 1.54j, 2024; https://imagej.net/ij/). The anatomical traits of vessels were studied quantitatively to investigate how a dry summer drives vessels' plasticity response to dry weather. Each vessel was assigned to one of the four domains, considering the position of its centre concerning domain boundaries in the tree-ring (Olano et al. 2022). The following anatomical traits, i.e. (i) mean vessel area (MVA), (ii) mean vessel diameter (MVD), (iii) vessel density (VD), and (iv) theoretical water conductive area (TWCA) were calculated for each sample tree (Figure 4) and finally averaged (Giagli et al. 2016; Prislan et al. 2018) according to Equations (4-7):

$$MVA (\mu m^2) = \frac{1}{n} \sum_{i=1}^{n} Va_i$$
 (4)

$$MVD (\mu m) = \frac{1}{n} \sum_{i=1}^{n} Vd_{i}$$
 (5)

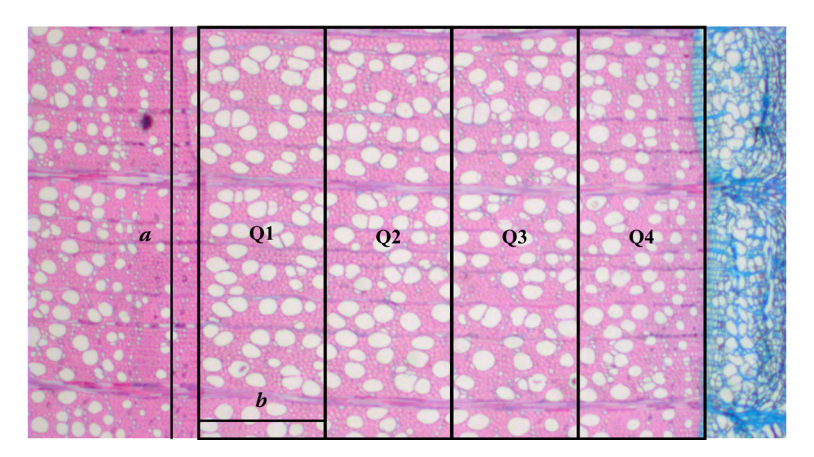


Figure 4. Schematic illustration of the analysed vessel traits in the quarter domains (Q1–Q4) of the xylem ring in the European beech microscopic sections

a – tangential width of the measured area; b – radial dimension of the measured area

$$TCWA (\%) = \frac{\sum_{i=1}^{n} Va_i}{a \times b} \times 100$$
 (6)

$$VD \text{ (No.·mm}^{-2}) = \frac{n}{a \times b}$$
 (7)

where:

n – number of vessels;

Vd – calculated vessel diameter based on the vessel area (Va) assuming a circular vessel lumen shape;

 a, b – tangential width and radial dimension of the measured area related to the *TRW*.

Data analysis. To check for significant differences within the vessel anatomical traits between the two age-class *F. sylvatica* stands, we used the non-parametric pairwise Mann–Whitney *t*-test. All statistical tests were performed using the Statistica 13.4.0.14 package (TIBCO Software Inc., USA). The mean values of each vessel's anatomy measurements in each domain (Q1–Q4) and *TRW* were calculated and used for analysis.

RESULTS

Timings of phenological phases of xylem formation. The cambium reactivation after the winter dormancy occurred within the second half of April (*DOY* 109–116). Soon after the onset

of the production of the first cambial cells, the first xylem elements (i.e. vessels) became distinguishable as thin-walled and non-lignified, post-cambial cells, as shown in Figure 3. The first enlargement cells (bE) appeared in the last week of April till the first week of May (DOY 116-123). The secondary wall thickening phase (bW) started approximately a week later (DOY 125-129) after the appearance of the first enlargement cells, while the first mature vessels (bM) were shown around four weeks later (DOY 151-152) at the end of May. The cambial cell activity, expressed through the enlargement phases (cE), ceased in both stands during the second half of July (DOY 193–202; Figure 5). After the cE phase, cell wall thickening and lignification continued for one month (DOY 222-225) and was completed from the beginning till the middle of August.

To test the differences between the two *F. sylvatica* stands, the timing and duration of phenological phase critical dates, expressed in *DOY*, were compared between the two age classes (Table 2).

No apparent differences were found among the spring phenological onset dates since the mean onset days of *bE*, *bW*, and *bM* were similar within age class. An approximately 10-day delay in the timing of the *cE* phase was observed in the younger age class of the *F. sylvatica* trees. Consequently, the *dE* period, i.e. the duration of cambial cell production expressed through the enlargement duration, was around a week longer in the young *F. sylvatica*

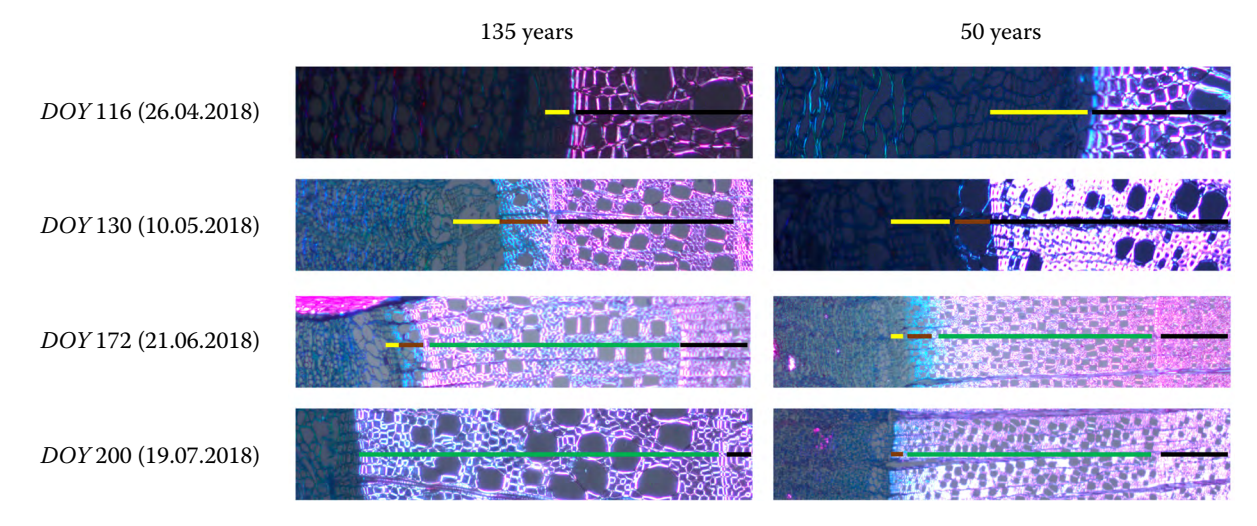


Figure 5. Polarised light microscope images of transverse sections in selected critical dates for the xylem formation of European beech trees, relevant to the four conceptual phenological phases: (i) Cambial division and (ii) enlargement zones (non-birefringent, yellow line), (iii) secondary wall thickening zone (birefringent blue and blue-red colour, dark orange line), (iv) mature zone (red colour, empty lumen, green line), and (v) previous year ring (black line)

DOY – day of the year

Table 2. Critical dates of phenological phases of xylem growth ring formation at the European beech forest stands during 2018, expressed in *DOY*

Age of the tree	bΕ	bW	bM	cE	cW	dE	dW	dX
135 years	118 ± 4	125 ± 4	151 ± 6	193 ± 6	222 ± 7	75 ± 4	97 ± 5	104 ± 5
50 years	121 ± 6	129 ± 5	152 ± 5	202 ± 8	225 ± 7	81 ± 7	96 ± 18	104 ± 16

DOY – day of the year, representing the mean values of the six trees per stand; bE – the onset of cell enlargement; bW – the onset of secondary wall thickening in vessels; bM – first mature vessels; cE – cessation of cell enlargement; cW – cessation of secondary wall formation and lignification; dE – duration of enlargement period; dW – duration of secondary wall thickening; dX – duration of xylem formation; '±' symbol – indication of standard deviation

trees. The mean DOY periods of dW and dX of the measured F. sylvatica trees were also similar in both stands. However, the younger F. sylvatica trees indicated higher variability in the dW and dX periods.

The first derivatives of each Gompertz function in each tree were calculated and then averaged to emphasise the differences in xylem increment widths during the growing season (Figure 6). Differences were also observed, as expected, in the daily growth rate increments. The mean rate width per active day during the growing season in each stand was $18.22~\mu m$ and $22.12~\mu m$ for the old- and

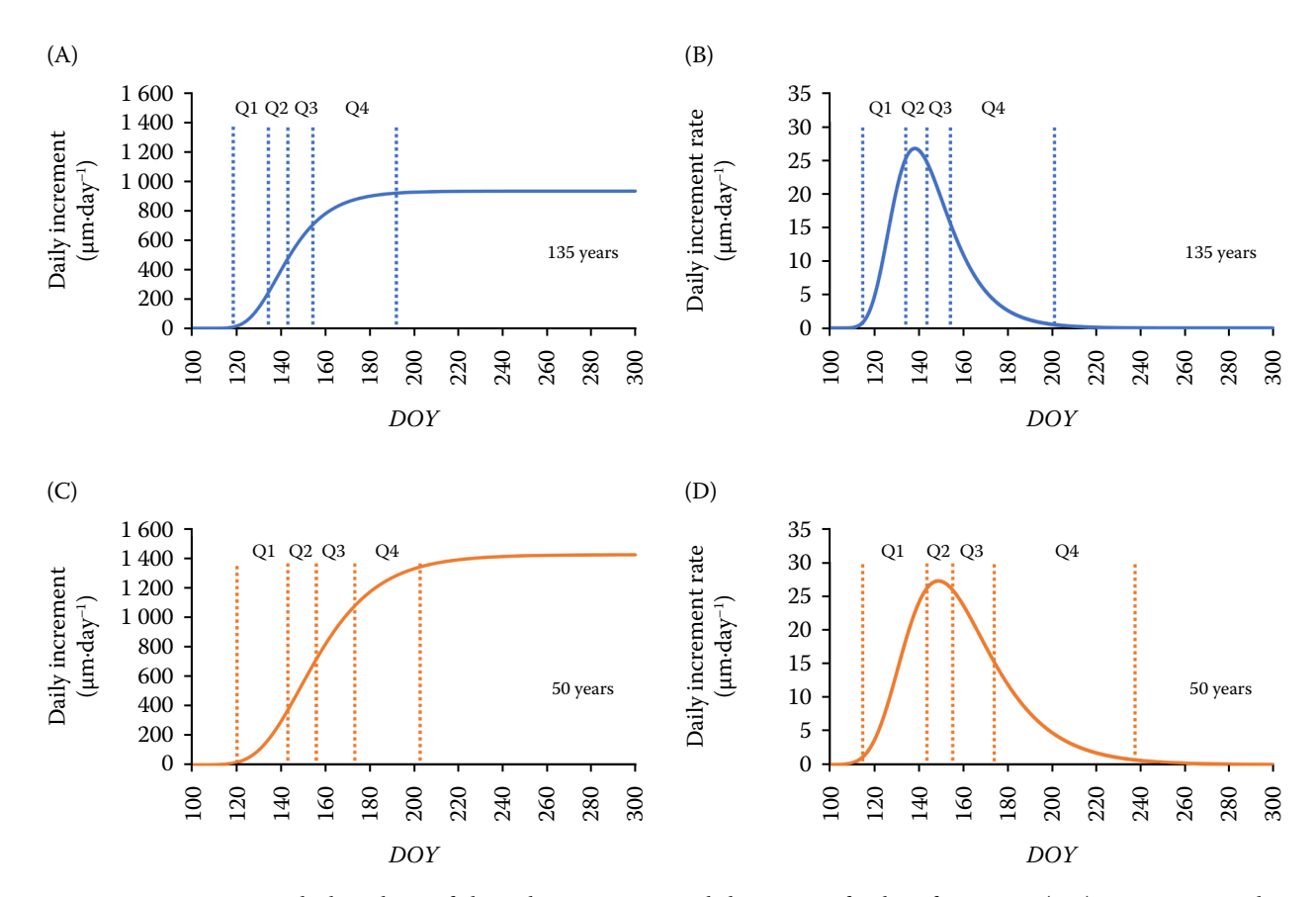


Figure 6. Formation and phenology of the xylem: Intra-annual dynamics of xylem formation (μ m), representing the mean cumulative increment of the six sampled trees at the selected European beech stands, i.e. the total ring increment comprised of enlarging, wall thickening and mature cells, during the growing season of 2018

DOY – day of the year; Q – xylem (TRW) increment quarter; TRW – tree-ring width;

The Gompertz function (left) fitted cumulative daily xylem growth curves; the mean first derivative of the Gompertz function was used to compare the extracted daily values with the theoretical incremental processes during the growing season (right); the peak of each first derivative function represents the time of the maximum width increment rate; the four divided quarters (domains) calculated according to the final tree ring growth increment are also depicted

Table 3. Dynamics of xylem formation as obtained from the mean Gompertz function parameters during the 2018 growing period

Parameters	135 years old	50 years old	
Final width increment (µm)	934.30	1 431.40	
Daily width rate (μm)	18.22	22.12	
Maximum daily width increment (μm)	26.81	27.39	
Day of maximum daily width increment (DOY)	138	148	
Duration of cambial cell activity (DOY)	52	72	

DOY - day of the year

young-age *F. sylvatica* trees, respectively. The mean maximum growth rate occurred earlier at the old age stand (*DOY* 138, May 18), while in the younger age trees at the end of the same month (*DOY* 148, May 28) according to the fitting model (Table 3).

As a result, different intra-annual growth patterns were observed during the studied year of 2018 (Figure 7), resulting in narrower tree rings in the older age-class F. sylvatica trees. The mean TRW of the old stand F. sylvatica trees was around 40% narrower (934.3 μ m) than the mean measured TRW of the young trees (1 431.4 μ m).

Vessel anatomical traits. Each *TRW* was divided into four equal domains (25% of the annual xy-

lem increment) to measure the vessels' anatomical traits. However, it should be noted that each quarter within each tree and age class was not identical since each *E. sylvatica* tree presented its growth rate and final *TRW* length, i.e. its annual xylem increments during its growing season. The main differences among the quarters were displayed between the Q1 and Q4 domains, i.e. close to the beginning and the cessation of the cambial cell production (enlargement phase period), in both ageclass stands (Table 4).

Vessel anatomical traits of MVA, MVD, and TWCA were relatively stable among the first three quarters and then essentially decreased in the fi-

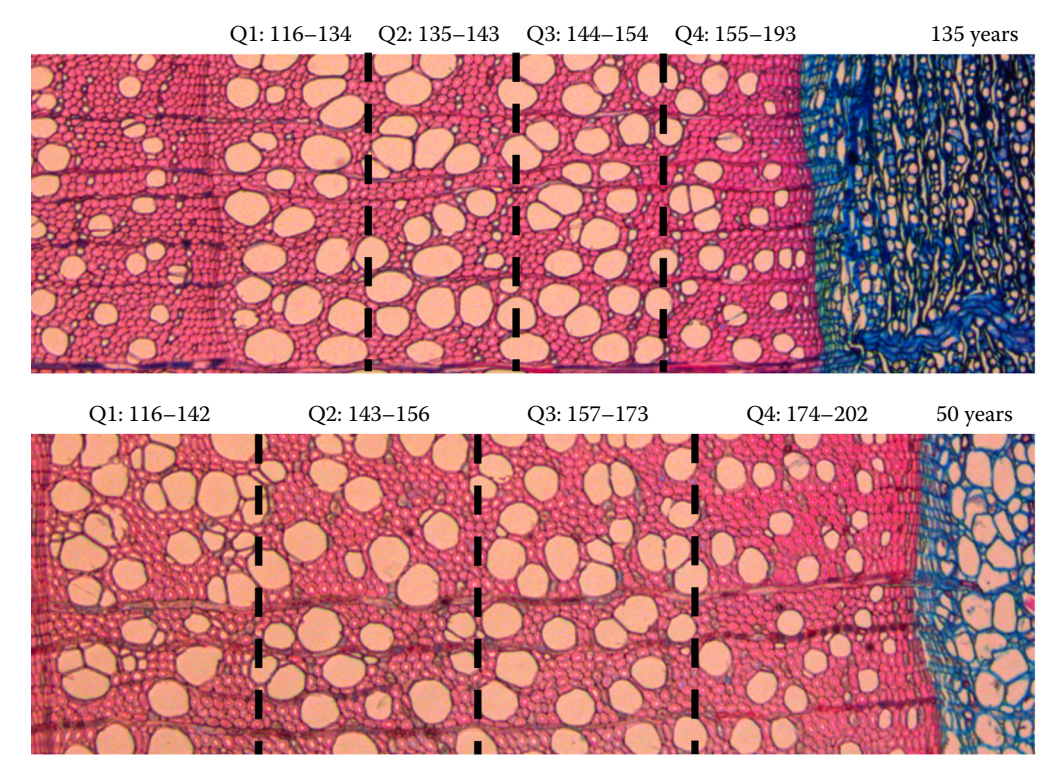


Figure 7. Fully formed annual tree-ring widths (TRWs) of the 135 and 50-year-old European beech trees; in each TRW, the quarter (Q1–Q4) domains and their duration period concerning the days of the year (DOY) are presented

Table 4. Descriptive mean values of vessel anatomical traits among the xylem increment quarters and between each age-class European beech stands

Quarter TRW	MVD (μm)		$MVA (\mu m^2)$		TWO	CA (%)	VD (No.·mm ⁻²)	
domain	135	50	135	50	135	50	135	50
Q1	65.1	58.7	2 762.5	2 330.1	28.8	30.1	105	131
	(± 7.1)	(± 3.6)	(± 478.4)	(± 284.6)	(± 7.0)	(± 5.5)	(± 27)	(± 14)
Q2	64.4	63.0	2 928.9	2 690.3	33.7	34.5	115	124
	(± 5.7)	(± 4.8)	(± 495.3)	(± 410.6)	(± 4.0)	(± 3.3)	(± 17)	(± 12)
Q3	60.0	59.6	2 555.4	2 540.4	31.3	30.8	128	125
	(± 6.7)	(± 4.4)	(± 519.4)	(± 407.5)	(± 3.1)	(± 3.1)	(± 16)	(± 9)
Q4	39.1	39.8	1 184.4	1 257.7	16.3	19.1	135	152
	(± 5.7)	(± 6.0)	(± 349.6)	(± 385.1)	(±5.7)	(± 6.7)	(± 23)	(± 27)
Q1-Q4	56.3	54.6	2 277.9	2 151.6	27.7	28.8	123	134
	(± 4.7)	(± 3.7)	(± 349.2)	(± 329.2)	(± 3.6)	(± 3.7)	(± 12)	(± 11)

Q - xylem (TRW) increment quarter; TRW - tree-ring width; MVD - mean vessel diameter; MVA - mean vessel area; TWCA - theoretical water conductive area; VD - vessel density; '±' symbol - standard deviation

nal Q4 *TRW* domain. *VD* (i.e. the number of vessels per mm²) indicated a slight increase in the Q4 domain. However, Mann–Whitney pairwise tests revealed no statistically significant differences between the two age-class *E. sylvatica* trees among the examined anatomical traits within each domain.

DISCUSSION

The summer conditions experienced in 2018 might have impaired the physiological integrity of many species, including F. sylvatica across Austria, Germany, Switzerland and other Central Europe regions (Schuldt et al. 2020; Dox et al. 2021; Rohner et al. 2021). Due to the higher T_{air} and VPD during the summer of 2018, evapotranspiration and soil water demand at the RAJ F. sylvatica trees were increased. Further, soil water availability was limited due to the low precipitation amount. Even though the drought intensity conditions were classified as moderate (-1.5 < SPEI < -1.0), the research area underwent a remarkable precipitation shortage within the two summer months of July and August. Drought can be aggravated by water shortage due to precipitation deficit and worsening drought conditions (Dai et al. 2018).

Timings of phenological phases of xylem formation. Late-successional species like F. sylvatica (Frouz et al. 2015) are believed to adopt safer life strategies, often associated with (i) ultimately higher growth rates and (ii) the spring photoperiod, while spring $T_{\rm air}$ becomes sensitive for the on-

set of cambial activity once the critical day length has been achieved (Cuny et al. 2012). Several studies underline the principal role of spring weather conditions, especially of T_{air} , on the cambial reactivation of F. sylvatica trees after winter dormancy (del Castillo et al. 2016; Kraus et al. 2016; D'Andrea et al. 2020). Dox et al. (2022) state that the mean 10-day $T_{\rm air}$ before cambial reactivation significantly affected the timing of cambial reactivation. The mean $T_{\rm air}$ at RAJ during this period (April 15–25) was 15.1 °C \pm 2.0 °C, while the first half of April (April 1-15) was relatively cold at 9.6 °C ± 3.8 °C. In this study, under the same weather conditions, we did not identify any difference in the timing of the cambial reactivation during the spring of 2018 between the two ageclass F. sylvatica trees. In both stands, the onset of cambial activity was estimated during the second half of April.

Regardless of age, most of the trees in this study ceased their enlargement by the end of July. This behaviour can be potentially attributed to the harsh environmental conditions the trees experienced this month. Unfavourable weather conditions, such as a dry summer, can reduce *F. sylvatica* growth (Dittmar et al. 2003; Giagli et al. 2016; Prislan et al. 2018). Xylem growth cessation can be strongly influenced by soil water availability, where dry conditions shortened the growing season by up to 25 days, regardless of the provenances of the *F. sylvatica* seedlings in a greenhouse experiment (Nielsen, Jørgensen 2003). Kraus et al. (2016)

concluded that warmer $T_{\rm air}$ could lengthen the tree-ring growth duration in F. sylvatica, under the assumption of no limitations due to drought stress. Yet, the factors that define cE are not considered simple like those for the bE. Late-season dynamics seem more subtle and complex and are influenced by the tree height, the diameter at breast height and tree age (Urban et al. 2014; Dox et al. 2022). Thus, the 10-day delayed cE noticed in the younger age trees can correlate with the age effect. Lignification of the last formed cells in this study ended around the middle of August (DOY 222-225) since it continues after the cessation of cambium activity for a few weeks to a maximum of 2 months until these cells mature (Oladi et al. 2011; Dox et al. 2021).

The end of the cell wall thickening phase seems to be a key date since it defines the end of xylem formation (del Castillo et al. 2016). Kraus et al. (2016) argued that the principal modulator is the end dates of xylem cell formation rather than the beginning dates or maximum growth rates. Likewise, Larysch et al. (2021) refer to the fact that the longer the growth duration is, the wider the tree ring, but they also found a significant positive linkage between growth rate and duration. In this study, the dX presented a mean growing season length of 104 days, which was relatively short, i.e. less than four months. On the other hand, this is not the first research to find such a short xylem growth season length, depending on the location and elevation of the studied sites. F. sylvatica trees have shown a shorter dX of 48–75 days in the south of Europe affected by Mediterranean climatic conditions (del Castillo et al. 2016), while Kraus et al. (2016) reported an average dX of 116 days in the Bavarian Alps. Likewise, Semeniuc et al. (2014) recorded an average dX duration of 127–137 days in the Rarău mountains (850 m a.s.l., Romania). Previous comparable studies in *F. sylvatica* trees at the RAJ reported a mean dE ranging from 85 to 106 days, which agrees with our results (Urban et al. 2014; Giagli et al. 2015; Giagli et al. 2016). In another research during 2018 in southwestern Germany (Larysch et al. 2021), cE and lignification on low elevation F. sylvatica sites occurred within the first week of August (DOY 217), approximately two to three weeks later than RAJ.

As expected, young-age trees displayed wider TRWs, and a higher maximum growth rate relevant to the old-age trees (H_1). In both stands, the

F. sylvatica had the steepest slope of ring growth from May to June, with the maximum growth rate marked at the DOY 138 (May 18) and 148 (May 28), for the old and young trees, respectively, supporting the strong influence of leaf phenology to F. sylvatica growth. The maximum growth rate usually varies between May and June, when leaf mass area and photosynthetic rate reach their maximum, due to the leaves' total development and most prolonged photoperiod duration till the summer solstice (Michelot et al. 2012; Urban et al. 2014). Our findings are in agreement with other studies (Čufar et al. 2008; Vavrčík et al. 2013; Semeniuc et al. 2014), that May and June (i) had the highest importance in radial growth, and (ii) tree-ring growth was mostly formed by the end of June.

Vessel anatomical traits. Xylem vulnerability to embolism resistance is a crucial parameter in understanding the drought resistance of trees, which (i) varies in tree populations according to their water availability, and (ii) can vary significantly between populations of the same species (Herbette et al. 2010). The mentioned vessel anatomical traits largely control the hydraulic properties of the conduits by modifying (phenotypic plasticity) the vessels' conductive efficiency (represented by MVA) and safety (represented by MVA and VD) of the water transport system (Oladi et al. 2014; Diaconu et al. 2016). Eilmann et al. (2014) stated that the wood structure of *F. sylvatica* trees is more strongly related to genetic predisposition than TRW and that genetic and environmental control interaction is generally low unless environmental extremes are considered. However, information about the genetic and phenotypic inter-annual variability of embolism resistance within species remains very scarce (Stojnić et al. 2018), and it is not sufficiently known whether trees of the same species follow the same adaptation strategy or how to control the number and the size of their water-conducting cells (Oladi et al. 2014). Considering the short geographical territory of the Czech Republic, the estimated genetic diversity found by Cvrčková et al. (2017) is not negligible; thus, it is essential to acquire more detailed knowledge about the dynamics of genetic diversity within and among beech populations.

Nevertheless, Stojnić et al. (2018) highlighted the importance of phenotypic plasticity among beech populations rather than genetic variations, as reported in other species, in embolism resistance. The intraspecific variability in xylem anatomy can

occur only in the growing season during xylem formation, with most genetic variations for most traits residing within populations. In contrast, environmental variations play a major role among *E. sylvatica* populations (Herbette et al. 2010) or provenances (Gričar et al. 2024).

Pairwise tests among the investigated vessel traits between the two age-class *F. sylvatica* trees located at RAJ indicated no statistically significant differences. This means that the mature trees (50 years and 135 years) studied showed no different patterns of intra-annual variability during the tree-ring growth period of xylem formation in 2018. Prislan et al. (2018) indicated that (i) the relationships among vessel traits can vary within a single ring, suggesting that the rate of vessel expansion at the beginning of the growing season may be more critical for the final vessel size than the duration of its expansion, and (ii) the only significant difference found among years and between F. sylvatica sites were in VD and not in MVA and/or TCWA. In addition, water transport in diffuse-porous beech does not rely only on the current xylem increment produced in each growing season as found in ringporous species but in several multiple growth rings (D'Andrea et al. 2020). There is a strong possibility of a time lag effect in the tree growth of the following year since diffuse-porous species like beech rely on the formed vessels of the previous year at the onset of cambial activity within the following spring (Bolte et al. 2007; Dox et al. 2021).

According to Arnič et al. (2021) and Gričar et al. (2024), dry weather conditions have been shown to affect beech wood structure, which is reflected in a change from a diffuse-porous to a semi-ring porous structure while MVA reached a maximum at 25% of the final TRW. Then, it was followed by a rapid decline in size. In this study, the MVA remained relatively constant in both age classes, up to 60%–80% of the final TRW, followed by a rapid drop only in the terminal part of the tree ring. Therefore, no apparent signs of summer drought stress could be detected in the vessel anatomy during the 2018 growing season in the RAJ for the measured F. sylvatica trees. A possible explanation is that radial growth was mostly completed by the end of July, and *F. sylvatica* trees might have adjusted the ending of xylem growth before stressful conditions occurred, as has been displayed for F. sylvatica trees growing in the Mediterranean region (D'Andrea et al. 2020). Even though PRCP deficits play a significant role in the likelihood of a tree/stand being affected, other parameters such as stand density or tree size, previous growth conditions (Rohner et al. 2021), silviculture treatments (Novák et al. 2017), the spatial edaphic pattern of forest ecosystem in general (Bulušek et al. 2016) are important too. In addition, Šimůnek et al. (2021) reported a close relationship between F, Sylvatica radial growth and solar activity besides $T_{\rm air}$ and annual PRCP.

CONCLUSION

European beech is considered among the most important economically hardwood species in the wood industry across Europe. It is well known to be rather sensitive to increased heatwaves and dry events. Thus, a better understanding of the phenological, physiological, and morphological beech tree mechanisms of European beech trees in a warmer climate is crucial for future forestry management practices. The 2018 warm and dry conditions during the summer period (July-August) and later on till the end of autumn resulted in a meteorological drought event with moderate severity (-1.5 < SPEI < -1.0). The tree-ring width length differences, as well as the maximum growth rates between the older (135 years) and younger age (50 years) beech stands, are a result of the age effect (H_1) . On the selected site, environmental factors seem to affect the beginning of xylem formation. Further, phenological phases such as the beginning of secondary wall formation or maturation and the duration of xylem formation were similar. Although our xylem formation findings do not thoroughly verify the idea of an age-dependent response to environmental conditions in the specific site, the relatively early cessation of cambial production, as expressed through the cessation of the enlargement phase combined with the observed time lag between the two age class trees, could be potentially assigned to the severe warm and dry conditions of July, and the age influence respectively (H_2) .

REFERENCES

Arnič D., Gričar J., Jevšenak J., Božič G., von Arx G., Prislan P. (2021): Different wood anatomical and growth responses in European beech (*Fagus sylvatica* L.) at three forest sites in Slovenia. Frontiers in Plant Science, 12: 669229.

- Battipaglia G., De Micco V., Sass-Klaassen U., Tognetti R., Mäkelä A. (2014): WSE symposium: Wood growth under environmental changes: The need for a multidisciplinary approach. Tree Physiology, 34: 787–791.
- Beeckman H. (2016): Wood anatomy and trait-based ecology. IAWA Journal, 37: 127–151.
- Boergens E., Güntner A., Dobslaw H., Dahle C. (2020): Quantifying the Central European droughts in 2018 and 2019 with GRACE Follow-On. Geophysical Research Letters, 47: e2020GL087285.
- Bolte A., Czajkowski T., Kompa T. (2007): The north-eastern distribution range of European beech A review. Forestry, 80: 413–429.
- Brázdil R., Zahradníček P., Dobrovolný P., Štěpánek P., Trnka M. (2021): Observed changes in precipitation during recent warming: The Czech Republic, 1961–2019. International Journal of Climatology, 41: 3881–3902.
- Broz A., Retallack G.J., Maxwell T.M., Silva L.C.R. (2021): A record of vapour pressure deficit preserved in wood and soil across biomes. Scientific Reports, 11: 662.
- Bulušek D., Vacek Z., Vacek S., Král J., Bílek L., Králíček I. (2016): Spatial pattern of relict beech (*Fagus sylvatica* L.) forests in the Sudetes of the Czech Republic and Poland. Journal of Forest Science, 62: 293–305.
- Cailleret M., Jansen S., Robert E.M.R., Desoto L., Aakala T., Antos J.A., Beikircher B., Bigler C., Bugmann H., Caccianiga M. et al. (2017): A synthesis of radial growth patterns preceding tree mortality. Global Change Biology, 23: 1675–1690.
- Cartenì F., Deslauriers A., Rossi S., Morin H., De Micco V., Mazzoleni S., Giannino F. (2018): The physiological mechanisms behind the earlywood-to-latewood transition: A process-based modelling approach. Frontiers in Plant Science, 9: 1053.
- Čermák P., Rybníček M., Žid T., Steffenrem A., Kolář T. (2019) Site and age-dependent responses of *Picea abies* growth to climate variability. European Journal of Forest Research, 138: 455–460.
- Charru M., Seynave I., Morneau F., Bontemps J.D. (2010): Recent changes in forest productivity: An analysis of national forest inventory data for common beech (*Fagus sylvatica* L.) in north-eastern France. Forest Ecology and Management, 260: 864–874.
- Chawla S., Nguyen V.X., Torres C.P.G., Pavelka M., Trusina J., Marek M.V. (2018): Wind characteristics recorded at the Czech Carbon Observation System (CzeCOS) site Rajec. European Journal of Environmental Sciences, 8: 117–123.
- Chen Y., Rademacher T., Fonti P., Eckes-Shephard A.H., LeMoine J.M., Fonti M.V., Richardson A.D., Friend A.D. (2022): Inter-annual and inter-species tree growth explained by phenology of xylogenesis. New Phytologist, 235: 939–952.
- Čufar K., Prislan P., de Luis M., Gričar J. (2008): Tree-ring variation, wood formation and phenology of beech (*Fagus*

- *sylvatica*) from a representative site in Slovenia, SE Central Europe. Trees, 22: 749–758.
- Cuny H.E., Rathgeber C.B.K., Lebourgeois F., Fortin M., Fournier M. (2012): Life strategies in intra-annual dynamics of wood formation: Example of three conifer species in a temperate forest in north-east France. Tree Physiology, 32: 612–625.
- Cvrčková H., Máchová P., Poláková L., Trčková O. (2017): Evaluation of the genetic diversity of selected *Fagus syl-vatica* L. populations in the Czech Republic using nuclear microsatellites. Journal of Forest Science, 63: 53–61.
- Dai A., Zhao T., Chen J. (2018): Climate change and drought: A precipitation and evaporation perspective. Current Climate Change Reports, 4: 301–312.
- D'Andrea E., Rezaie N., Prislan P., Gričar J., Collalti A., Muhr J., Matteucci G. (2020): Frost and drought: Effects of extreme weather events on stem carbon dynamics in a Mediterranean beech forest. Plant, Cell & Environment, 43: 2365–2379.
- Del Castillo E.M., Longares L.A., Gričar J., Prislan P., Gil-Pelegrin E., Čufar K., de Luis M. (2016): Living on the edge: Contrasted wood-formation dynamics in *Fagus sylvatica* and *Pinus sylvestris* under Mediterranean conditions. Frontiers in Plant Science, 7: 370.
- De Micco V., Carrer M., Rathgeber C.B.K., Camarero J.J., Voltas J., Cherubini P., Battipaglia G. (2019): From xylogenesis to tree rings: Wood traits to investigate tree response to environmental changes. IAWA Journal, 40: 155–182.
- Deslauriers A., Morin H., Begin Y. (2003): Cellular phenology of annual ring formation of *Abies balsamea* in the Quebec boreal forest (Canada). Canadian Journal of Forest Research, 33: 190–200.
- Deslauriers A., Fonti P., Rossi S., Rathgeber C.B.K., Gričar J. (2018): Ecophysiology and plasticity of wood and phloem formation. In: Amoroso M.M., Daniels L.D., Baker P.J., Camarero J.J. (eds): Dendroecology. Tree-ring Analyses Applied to Ecological Studies. Cham, Springer International Publishing: 13–34.
- Diaconu D., Stangler D.F., Kahle H.P., Spiecker H. (2016): Vessel plasticity of European beech in response to thinning and aspect. Tree Physiology, 36: 1260–1271.
- Diaconu D., Hackenberg J., Stangler D.F., Kahle H.P., Spiecker H. (2017): Simulation study to determine necessary sample sizes for image analysis-based quantitative wood anatomy of vessels of beech (*Fagus sylvatica*). Dendrochronologia, 45: 35–38.
- Dittmar C., Zech W., Elling W. (2003): Growth variations of common beech (*Fagus sylvatica* L.) under different climatic and environmental conditions in Europe A dendroecological study. Forest Ecology and Management, 173: 63–78.
- Dorado-Liñán I., Gutiérrez E., Heinrich I., Andreu-Hayles L., Muntán E., Campelo F., Helle G. (2012): Age effects and

- climate response in trees: A multi-proxy tree-ring test in old-growth life stages. European Journal of Forest Research, 131: 933–944.
- Dox I., Prislan P., Gričar J., Mariën B., Delpierre N., Flores O., Leys S., Rathgeber C.B.K., Fonti P., Campioli M. (2021): Drought elicits contrasting responses on the autumn dynamics of wood formation in late successional deciduous tree species. Tree Physiology, 41: 1171–1185.
- Dox I., Mariën B., Zuccarini P., Marchand L.J., Prislan P., Gričar J., Flores O., Gehrmann F., Fonti P., Lange H., Peñuelas J., Campioli M. (2022): Wood growth phenology and its relationship with leaf phenology in deciduous forest trees of the temperate zone of Western Europe. Agricultural and Forest Meteorology, 327: 109229.
- Eilmann B., Sterck F., Wegner L., de Vries S.M.G., von Arx G., Mohren G.M.J., den Ouden J., Sass-Klaassen U. (2014): Wood structural differences between northern and southern beech provenances growing at a moderate site. Tree Physiology, 34: 882–893.
- Fonti P., Babushkina E.A. (2016): Tracheid anatomical responses to climate in a forest-steppe in Southern Siberia. Dendrochronologia, 39: 32–41.
- Frouz J., Vobořilová V., Janoušová I., Kadochová Š., Matějíček L. (2015): Spontaneous establishment of late successional tree species English oak (*Quercus robur*) and European beech (*Fagus sylvatica*) at reclaimed alder plantation and unreclaimed post mining sites. Ecological Engineering, 77: 1–8.
- Geletič J., Lehnert M., Dobrovolný P., Žuvela-Aloise M. (2019): Spatial modelling of summer climate indices based on local climate zones: Expected changes in the future climate of Brno, Czech Republic. Climate Change, 152: 487–502.
- Genet H., Bréda N., Dufrêne E. (2010): Age-related variation in carbon allocation at tree and stand scales in beech (*Fagus sylvatica* L.) and sessile oak (*Quercus petraea* (Matt.) Liebl.) using a chronosequence approach. Tree Physiology, 30: 177–192.
- Giagli K., Veteška O., Vavrčík H., Gryc V. (2015): Monitoring of seasonal dynamics in two age-different European beech stands. Wood Research, 60: 1005–1016.
- Giagli K., Gričar J., Vavrčík H., Menšík L., Gryc V. (2016): The effects of drought on wood formation in *Fagus sylvatica* during two contrasting years. IAWA Journal, 37: 332–348.
- Gričar J., Prislan P., Gryc V., Vavrčík H., de Luis M., Čufar K. (2014): Plastic and locally adapted phenology in cambial seasonality and production of xylem and phloem cells in *Picea abies* from temperate environments. Tree Physiology, 34: 869–881.
- Gričar J., Arnič D., Krajnc L., Prislan P., Božič G., Westergren M., Mátyás C., Kraigher H. (2024): Different patterns of inter-annual variability in mean vessel area and tree-ring

- widths of beech from provenance trials in Slovenia and Hungary. Trees, 38: 179–195.
- Hartmann F.P., Rathgeber C.B.K., Fournier M., Moulia B. (2017): Modelling wood formation and structure: Power and limits of a morphogenetic gradient in controlling xylem cell proliferation and growth. Annals of Forest Science, 74: 14.
- Herbette S., Wortemann R., Awad H., Huc R., Cochard H., Barigah T.S. (2010): Insights into xylem vulnerability to cavitation in *Fagus sylvatica* L.: Phenotypic and environmental sources of variability. Tree Physiology, 30: 1448–1455.
- Hoylman Z.H., Jencso K.G., Hu J., Holden Z.A., Martin J.T., Gardner W.P. (2019): The climatic water balance and topography control spatial patterns of atmospheric demand, soil moisture and shallow subsurface flow. Water Resources Research, 55: 2370–2389.
- Ježík M., Blaženec M., Kučera J., Střelcová K., Ditmarová L. (2016): The response of intra-annual stem circumference increase of young European beech provenances to 2012–2014 weather variability. iForest, 9: 960–969.
- Kolář T., Giagli K., Trnka M., Bednářová E., Vavrčík H., Rybníček M. (2016): Response of the leaf phenology and tree-ring width of European beech to climate variability. Silva Fennica, 50: 1520.
- Kraus C., Zang C., Menzel A. (2016): Elevational responses in leaf and xylem phenology reveals different prolongation of growing period of common beech and Norway spruce under warming conditions in the Bavarian Alps. European Journal of Forest Research, 135: 1011–1023.
- Larysch E., Stangler D.F., Nazari M., Seifert T., Kahle H.P. (2021): Xylem phenology and growth response of European beech, silver fir and Scots pine along an elevational gradient during the extreme drought year 2018. Forests, 12: 75.
- Leuschner C. (2020): Drought response of European beech (*Fagus sylvatica* L.) A review. Perspectives in Plant Ecology, Evolution and Systematics, 47: 125576.
- Li X., Liang E., Gričar J., Prislan P., Rossi S., Čufar K. (2013): Age dependence of xylogenesis and its climatic sensitivity in Smith fir on the south-eastern Tibetan Plateau. Tree Physiology, 33: 48–56.
- Matisons R., Krišāns O., Kārkliņa A., Adamovičs A., Jansons Ā., Gärtner H. (2019): Plasticity and climatic sensitivity of wood anatomy contribute to performance of eastern Baltic provenances of Scots pine. Forest Ecology and Management, 452: 117568.
- McGloin R., Šigut L., Fischer M., Foltýnová L., Chawla S., Trnka M., Pavelka M., Marek M.V. (2019): Available energy partitioning during drought at two Norway spruce forests and a European beech forest in Central Europe. Journal of Geophysical Research: Atmospheres, 124: 3726–3742.
- Mesbahzadeh T., Mirakbari M., Saravi M.M., Sardoo F.S., Miglietta M.M. (2020): Meteorological drought analysis using

- copula theory and drought indicators under climate change scenarios (RCP). Meteorological Applications, 27: e1856.
- Michelot A., Simard S., Rathgeber C., Dufrêne E., Damesin C. (2012): Comparing the intra-annual wood formation of three European species (*Fagus sylvatica*, *Quercus petraea* and *Pinus sylvestris*) as related to leaf phenology and non-structural carbohydrate dynamics. Tree Physiology, 32: 1033–1043.
- Nielsen C.N., Jørgensen F.V. (2003): Phenology and diameter increment in seedlings of European beech (*Fagus sylvatica* L.) as affected by different soil water contents: Variation between and within provenances. Forestry Ecology and Management, 174: 233–249.
- Novák J., Dušek D., Slodičák M., Kacálek D. (2017): Importance of the first thinning in young mixed Norway spruce and European beech stands. Journal of Forest Science, 63: 254–262.
- Oladi R., Pourtahmasi K., Eckstein D., Bräuning A. (2011): Seasonal dynamics of wood formation in Oriental beech (*Fagus orientalis* Lipsky) along an altitudinal gradient in the Hyrcanian forest, Iran. Trees, 25: 425–433.
- Oladi R., Bräuning A., Pourtahmasi K. (2014): 'Plastic' and 'static' behavior of vessel-anatomical features in Oriental beech (*Fagus orientalis* Lipsky) in view of xylem hydraulic conductivity. Trees, 28: 493–502.
- Olano J.M., Hernández-Alonso H., Sangüesa-Barreda G., Rozas V., García-Cervigón A.I., García-Hidalgo M. (2022): Disparate response to water limitation for vessel area and secondary growth along *Fagus sylvatica* southwestern distribution range. Agricultural and Forest Meteorology, 323: 109082.
- Parente J., Amraoui M., Menezes I., Pereira M.G. (2019): Drought in Portugal: Current regime, comparison of indices and impacts on extreme wildfires. Science of the Total Environment, 685: 150–173.
- Plomion C., Leprovost G., Stokes A. (2001): Wood formation in trees. Plant Physiology, 127: 1513–1523.
- Pourtahmasi K., Lotfiomran N., Bräuning A., Parsapajouh D. (2011): Tree-ring width and vessel characteristics of oriental beech (*Fagus orientalis*) along an altitudinal gradient in the Caspian forests, northern Iran. IAWA Journal, 32: 461–473.
- Prislan P., Gričar J., de Luis M., Smith K.T., Čufar K. (2013): Phenological variation in xylem and phloem formation in *Fagus sylvatica* from two contrasting sites. Agricultural and Forest Meteorology, 180: 142–151.
- Prislan P., Čufar K., de Luis M., Gričar J. (2018): Precipitation is not limiting for xylem formation dynamics and vessel development in European beech from two temperate forest sites. Tree Physiology, 38: 186–197.
- Prislan P., Gričar J., Čufar K., de Luis M., Merela M., Rossi S. (2019): Growing season and radial growth predicted for *Fagus sylvatica* under climate change. Climatic Change, 153: 181–197.

- Prislan P., del Castillo E.M., Skoberne G., Špenko N., Gričar J. (2022): Sample preparation protocol for wood and phloem formation analyses. Dendrochronologia, 73: 125959.
- Rathgeber C.B.K., Longuetaud F., Mothe F., Cuny H., Le Moguédec G. (2011): Phenology of wood formation: Data processing, analysis and visualisation using R (package CAVIAR). Dendrochronologia, 29: 139–149.
- Rathgeber C.B.K., Cuny H.E., Fonti P. (2016): Biological basis of tree-ring formation: A crash course. Frontiers in Plant Science, 7: 734.
- Rathgeber C.B.K., Santenoise P., Cuny H.E. (2018): CAVIAR: An R package for checking, displaying and processing woodformation-monitoring data. Tree Physiology, 38: 1246–1260.
- Rodriguez-Zaccaro F.D., Valdovinos-Ayala J., Percolla M.I., Venturas M.D., Pratt R.B., Jacobsen A.L. (2019): Wood structure and function change with maturity: Age of the vascular cambium is associated with xylem changes in current-year growth. Plant Cell and Environment, 42: 1816–1831.
- Rohner B., Kumar S., Liechti K., Gessler A., Ferretti M. (2021): Tree vitality indicators revealed a rapid response of beech forests to the 2018 drought. Ecological Indicators, 120: 106903.
- Rossi S., Deslauriers A., Morin H. (2003): Application of the Gompertz equation for the study of xylem cell development. Dendrochronologia, 21: 33–39.
- Rossi S., Deslauriers A., Anfodillo T. (2006): Assessment of cambial activity and xylogenesis by microsampling tree species: An example at the alpine timberline. IAWA Journal, 27: 383–394.
- Rossi S., Deslauriers A., Anfodillo T., Carrer M. (2008): Age-dependent xylogenesis in timberline conifers. New Phytologist, 177: 199–208.
- Ryan M.G., Binkley D., Fownes J.H. (1997): Age-related decline in forest productivity: Pattern and process. In: Begon M., Fitter A.H. (eds): Advances in Ecological Research, Volume 27. San Diego, Academic Press: 213–262.
- Sass U., Eckstein D. (1995): The variability of vessel size in beech (*Fagus sylvatica* L.) and its ecophysiological interpretation. Trees, 9: 247–252.
- Schuldt B., Buras A., Arend M., Vitasse Y., Beierkuhnlein C., Damm A., Gharun M., Grams T.E.E., Hauck M., Hajek P. et al. (2020): A first assessment of the impact of the extreme 2018 summer drought on Central European forests. Basic and Applied Ecology, 45: 86–103.
- Semeniuc A., Popa I., Timofte A.I., Gurean D.M. (2014): Xylem phenology of *Fagus sylvatica* in Rarău mountains (Eastern Carpathians, Romania). Notulae Botanicae Horti Agrobotanici Cluj-Napoca, 42: 275–279.
- Šimůnek V., Hájek V., Prokůpková A., Gallo J. (2021): Finding an imprint of solar and climatic cycles in tree rings of European beech (*Fagus sylvatica* L.). Journal of Forest Science, 67: 409–419.

- Skalák P., Štěpánek P., Zahradníček P., Trnka M. (2019): Extreme drought of 2018 in the Czech Republic. In: Geophysical Research Abstracts: 21st EGU General Assembly, Volume 21, Vienna, Apr 7–12, 2019: EGU2019-11262.
- Stojnić S., Suchocka M., Benito-Garzón M., Torres-Ruiz J.M., Cochard H., Bolte A., Cocozza C., Cvjetković B., de Luis M., Martinez-Vilalta J., Ræbild A., Tognetti R., Delzon S. (2018): Variation in xylem vulnerability to embolism in European beech from geographically marginal populations. Tree Physiology, 38: 173–185.
- Urban J., Bednářová E., Plichta R., Gryc V., Vavrčík H., Hacura J., Fajstavr M., Kučera J. (2014): Links between phenology and ecophysiology in a European beech forest. iForest, 8: 438–447.
- Vavrčík H., Gryc V., Menšík L., Baar J. (2013): Xylem formation in *Fagus sylvatica* during one growing season. Dendrobiology, 69: 69–75.

- Vicente-Serrano S.M., Beguería S., López-Moreno J. (2010): A multiscalar drought index sensitive to global warming: The standardized precipitation evapotranspiration index. Journal of Climate, 23: 1696–1718.
- Vieira J., Carvalho A., Campelo F. (2020): Tree growth under climate change: Evidence from xylogenesis timings and kinetics. Frontiers in Plant Science, 11: 90.
- Wilson B.F., Wodzicki T.J., Zahner R. (1966): Differentiation of cambial derivatives: Proposed terminology. Forest Science, 12: 438–440.
- Zeng Q., Rossi S., Yang B. (2018): Effects of age and size on xylem phenology in two conifers of northwestern China. Frontiers in Plant Science, 8: 2264.

Received: February 22, 2024 Accepted: June 6, 2024 Published online: September 6, 2024